Robotics 1

February 16, 2024

Exercise 1

With reference to Fig. 1, a PPR planar robot with a third link of length ℓ has to pick up with its end-effector gripper an object that is localized by the views of two co-planar cameras C_1 and C_2. Although living in 3D, this visual localization problem can be essentially restricted to the plane $(\boldsymbol{x}_b, \boldsymbol{y}_b)$ of the reference frame placed at the robot base. Each camera $(i = 1, 2)$ is represented by a pinhole model with focal length f_i and a reference frame placed on its image plane, having the $\boldsymbol{z}_{ci}$ axis along the optical axis and the $\boldsymbol{x}_{ci}$ axis in the same plane $(\boldsymbol{x}_b, \boldsymbol{y}_b)$. The pose of these two camera frames is known with respect to the base frame of the robot, using the geometric parameters L, H, α_1, and α_2 defined in the figure.

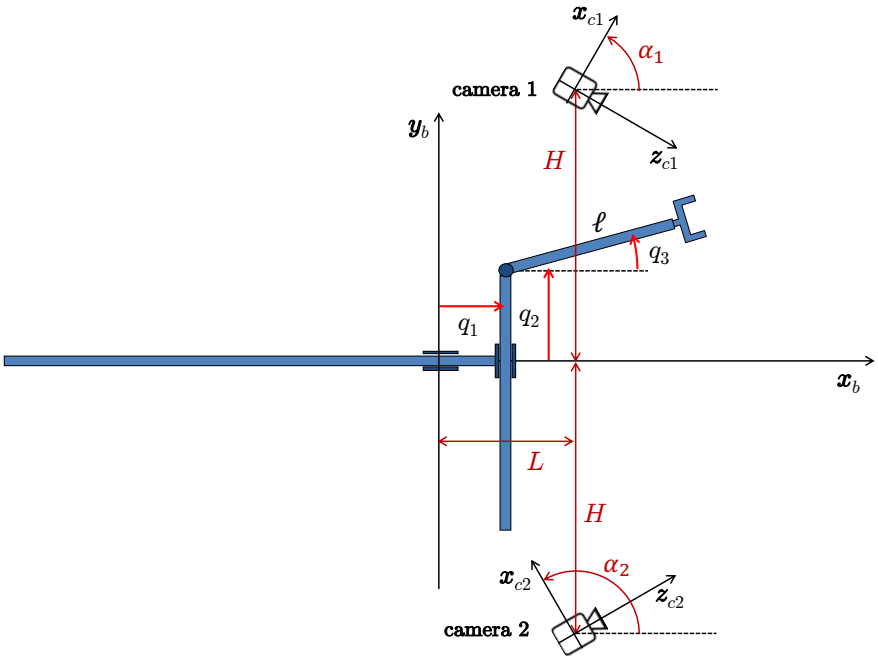

Figure 1: The planar setup of the visual localization problem, with two cameras and a PPR robot.

A point feature P on the object is seen in the image plane of camera C_1 at a signed distance d_1 along its $\boldsymbol{x}_{c1}$ axis, while the same feature is seen by camera C_2 at a signed distance d_2 along its $\boldsymbol{x}_{c2}$ axis.[1] Both d_1 and d_2 are expressed in metric units (i.e., neglecting pixelation).

a) Find the position ${}^{ci}\boldsymbol{p}$ of the point feature P in one of the camera frames — any, $i = 1$ or 2 (or in both).

b) Determine the position of P as ${}^{b}\boldsymbol{p}$, i.e., with respect to the reference frame at the base of the robot.

c) Provide the numerical value of ${}^{b}\boldsymbol{p}$ when using the following data: $\ell = 0.5$, $L = 0.4$, and $H = 0.8$ [m]; $\alpha_1 = \pi/3$ and $\alpha_2 = 2\pi/3$ [rad]; $f_1 = 10$ and $f_2 = 12$ [mm]; $d_1 = 6$ and $d_2 = -2$ [mm].

d) Find a closed form solution of the inverse kinematics problem for the PPR robot, when the planar position and orientation of its end-effector are given. Is the solution unique?

e) Provide a numerical value of the joint variable vector $\boldsymbol{q} = (q_1, q_2, q_3)$ for the position ${}^{b}\boldsymbol{p}$ and the data in item c), when the robot end-effector points toward the origin of the camera frame in C_2.

[1] We assume that the correspondence problem between the two images has been solved already.

Exercise 2

A 3-dof cylindrical robot is shown in Fig. 2.

a) Assign the frames according to the Denavit-Hartenberg (D-H) convention, so that all constant D-H parameters are non-negative. Provide the table with the corresponding parameters. The first frame should be placed on the floor at the robot base and the origin of the last frame should be at point P. Compute position and orientation of the end-effector frame as given by the homogeneous matrix ${}^0\boldsymbol{T}_3(\boldsymbol{q})$.

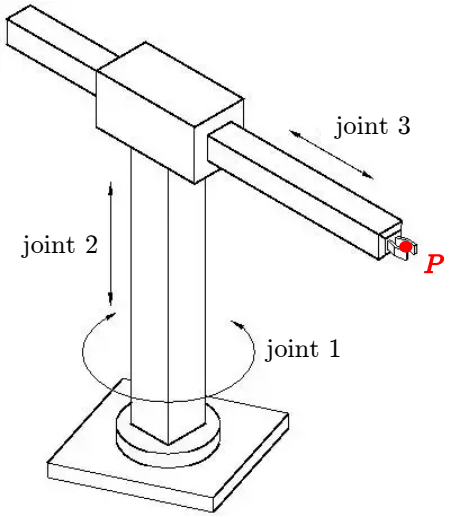

Figure 2: A 3-dof cylindrical robot.

b) For a desired position $\boldsymbol{p}_d \in \mathbb{R}^3$ of the end-effector, find all solutions to the inverse kinematics problem.

c) Sketch the primary workspace of this robot, when $q_1 \in [-5\pi/6, 5\pi/6]$, $q_2 \in [0, H]$, and $q_3 \in [D_{min}, D_{max}]$, with $D_{min} > 0$. How many inverse kinematics solutions may comply with these bounds?

d) Compute the 3×3 Jacobian matrix $\boldsymbol{J}(\boldsymbol{q})$ relating $\dot{\boldsymbol{q}}$ to the velocity $\boldsymbol{v}$ of point P and find its singularities.

e) When the Jacobian is evaluated at a generic singular configuration $\boldsymbol{q}_s$, find a basis for the two subspaces $\mathcal{N}(\boldsymbol{J}_s)$ and $\mathcal{N}(\boldsymbol{J}_s^T)$, where $\boldsymbol{J}_s = \boldsymbol{J}(\boldsymbol{q}_s)$. Provide a physical interpretation of the vectors belonging to each of these two subspaces.

Exercise 3

Consider the following trajectory planning problem for a 2R planar robot with links of length $L_1 = 2$ and $L_2 = 1$ [m]. The robot should perform a rest-to-rest motion in a given time $T = 2$ s, moving its end-effector from point $A = (0, 1)$ to point $B = (3, 0)$ [m]. The initial direction of the end-effector motion from point A is specified by the tangent vector in Cartesian space $d\boldsymbol{p}/ds|_A = (5, 0)$, where s is a suitable scalar that parametrizes the path. Similarly, the final approach direction to point B is specified by $d\boldsymbol{p}/ds|_B = (0, -1)$.

a) Design a joint trajectory that solves this problem, providing the analytic expression of the various terms in the complete solution and some plots that help illustrating it.

b) Suppose now that the joint velocities are limited: $|\dot{q}_1| \leq V_1 = 2$, $|\dot{q}_2| \leq V_2 = 3$ [rad/s]. Verify whether the trajectory that has been planned in item a) is feasible. If this is not the case, determine a convenient, possibly minimum, motion time T^* that solves the same problem and complies also with these bounds.

Exercise 4

The kinematics of a 3R spatial robot is specified through the D-H parameters given in Tab. 1. The robot has its base mounted on the floor, defined by the plane $(\boldsymbol{x}_0, \boldsymbol{y}_0)$.

i	α_i	a_i	d_i	θ_i
1	$\pi/2$	0	0.7	q_1
2	0	0.5	0	q_2
3	0	0.5	0	q_3

Table 1: D-H parameters of a 3R spatial robot (lengths are in [m]).

The desired trajectory of the robot end-effector is an helical path to be traced, for $t \in [0, 3]$, with constant parametric speed $\dot{s} = v$:

$$\begin{aligned} p_{x,d}(t) &= r \cos 2\pi s(t) \\ p_{y,d}(t) &= r \sin 2\pi s(t) \\ p_{z,d}(t) &= h_0 + hs(t), \end{aligned} \tag{1}$$

with $r = 0.5$, $h_0 = 0.2$, and $h = 0.4$ [m], and $v = 1$ [s^{-1}]. The robot is commanded by the joint velocity vector $\dot{\boldsymbol{q}} \in \mathbb{R}^3$ and has unlimited joint rotations.

a) Show that the entire desired trajectory $\boldsymbol{p}_d(t) \in \mathbb{R}^3$ belongs to the primary workspace of the robot and that it can be traced without encountering any singular configuration.

b) With the robot starting at $t = 0$ from the initial configuration $\boldsymbol{q}(0) = (0, \pi/6, -\pi/2)$ [rad], verify whether the end-effector is on the desired trajectory or not.

c) Design a kinematic control law that achieves tracking of the desired end-effector trajectory, with the possible position error $\boldsymbol{e} \in \mathbb{R}^3$ decaying exponentially, so that the error components $e_i(t)$, $i = t, n, b$, are decoupled in the Frenet frame $(\boldsymbol{t}, \boldsymbol{n}, \boldsymbol{b})$ associated to the desired position along the path.

d) Wishing to impose the error dynamics $\dot{e}_t = -2e_t$, $\dot{e}_n = -5e_n$, $\dot{e}_b = -5e_b$, compute at $t = 0$ the numerical value of the command $\dot{\boldsymbol{q}}(0)$ when the robot starts from the configuration of item b) and the control law in item c) is being used.

[5 hours; open books]

Solution

February 16, 2024

Exercise 1

We first define the relationships between the different frames of interest. The two camera frames are related to the base frame of the robot, respectively by

$$ {}^{b}\boldsymbol{T}_{c1} = \begin{pmatrix} \cos\alpha_1 & 0 & \sin\alpha_1 & L \\ \sin\alpha_1 & 0 & -\cos\alpha_1 & H \\ 0 & 1 & 0 & 0 \\ 0 & 0 & 0 & 1 \end{pmatrix}, \qquad {}^{b}\boldsymbol{T}_{c2} = \begin{pmatrix} \cos\alpha_2 & 0 & \sin\alpha_2 & L \\ \sin\alpha_2 & 0 & -\cos\alpha_2 & -H \\ 0 & 1 & 0 & 0 \\ 0 & 0 & 0 & 1 \end{pmatrix}, \tag{2} $$

so that the pose of the second camera is expressed in the first camera frame by

$$ {}^{c1}\boldsymbol{T}_{c2} = {}^{b}\boldsymbol{T}_{c1}^{-1}\,{}^{b}\boldsymbol{T}_{c2} = \begin{pmatrix} \cos(\alpha_1-\alpha_2) & 0 & -\sin(\alpha_1-\alpha_2) & -2H\sin\alpha_1 \\ 0 & 1 & 0 & 0 \\ \sin(\alpha_1-\alpha_2) & 0 & \cos(\alpha_1-\alpha_2) & 2H\cos\alpha_1 \\ 0 & 0 & 0 & 1 \end{pmatrix}. $$

Note that the parameter L disappears from this matrix.

Let ${}^{ci}P = (X_i, Z_i)$ be the coordinates (in the plane) of the feature point P as seen in the i-th camera frame, for $i = 1, 2$. Using the pinhole model, and taking into account that the camera frames are placed on their respective image plane, we have the perspective relations

$$ \frac{f_i}{d_i} = -\frac{Z_i - f_i}{X_i} \qquad \Rightarrow \qquad f_i X_i + d_i Z_i = d_i f_i, \qquad i = 1, 2. \tag{3} $$

Embedding the point P in homogeneous coordinates, we have

$$ {}^{c1}\boldsymbol{p}_{hom} = \begin{pmatrix} {}^{c1}\boldsymbol{p} \\ 1 \end{pmatrix} = \begin{pmatrix} X_1 \\ 0 \\ Z_1 \\ 1 \end{pmatrix} \qquad {}^{c2}\boldsymbol{p}_{hom} = \begin{pmatrix} {}^{c2}\boldsymbol{p} \\ 1 \end{pmatrix} = \begin{pmatrix} X_2 \\ 0 \\ Z_2 \\ 1 \end{pmatrix}. $$

Thus, from

$$ {}^{c1}\boldsymbol{p}_{hom} = {}^{c1}\boldsymbol{T}_{c2}\,{}^{c2}\boldsymbol{p}_{hom} $$

one has in particular

$$ \begin{aligned} X_1 &= X_2\cos(\alpha_1-\alpha_2) - Z_2\sin(\alpha_1-\alpha_2) - 2H\sin\alpha_1 \\ Z_1 &= X_2\sin(\alpha_1-\alpha_2) + Z_2\cos(\alpha_1-\alpha_2) + 2H\cos\alpha_1. \end{aligned} \tag{4} $$

Substituting (4) in the first of the two perspective relations (3), we obtain the following 2×2 system of linear equations in the unknowns X_2 and Z_2:

$$ \boldsymbol{A}\begin{pmatrix} X_2 \\ Z_2 \end{pmatrix} = \boldsymbol{b}, \tag{5} $$

with

$$ \begin{aligned} \boldsymbol{A} &= \begin{pmatrix} f_1\cos(\alpha_1-\alpha_2) + d_1\sin(\alpha_1-\alpha_2) & -f_1\sin(\alpha_1-\alpha_2) + d_1\cos(\alpha_1-\alpha_2) \\ f_2 & d_2 \end{pmatrix} \\ \boldsymbol{b} &= \begin{pmatrix} d_1 f_1 + 2H(f_1\sin\alpha_1 - d_1\cos\alpha_1) \\ d_2 f_2 \end{pmatrix}. \end{aligned} $$

Except for singular cases (here ruled out by the placement of the two cameras), the 'triangulation' system (5) is solvable and provides the localization of the point feature P in the frame of the second camera. Substituting the data,[2] we have

$$\boldsymbol{A} = \begin{pmatrix} -0.000196 & 0.011660 \\ 0.012 & -0.002 \end{pmatrix} \qquad \boldsymbol{b} = \begin{pmatrix} 0.009116 \\ -0.000024 \end{pmatrix},$$

and so

$${}^{c2}P = \begin{pmatrix} X_2 \\ Z_2 \end{pmatrix} = \boldsymbol{A}^{-1}\boldsymbol{b} = \begin{pmatrix} 0.1287 \\ 0.7840 \end{pmatrix} \text{ [m]}. \tag{6}$$

From eq. (4) we get also the localization of the point feature P in the frame of the second camera

$${}^{c1}P = \begin{pmatrix} X_1 \\ Z_1 \end{pmatrix} = \begin{pmatrix} -0.6423 \\ 1.0806 \end{pmatrix} \text{ [m]}. \tag{7}$$

Finally, we localize the point feature P in the base frame of the robot, i.e., compute ${}^{b}P = (X_b, Y_b)$, using any of the two camera transformations in (2), together with (6) or (7);

$${}^{b}\boldsymbol{p}_{hom} = {}^{b}\boldsymbol{T}_{c1}\,{}^{c1}\boldsymbol{p}_{hom} = {}^{b}\boldsymbol{T}_{c2}\,{}^{c2}\boldsymbol{p}_{hom} \qquad \Rightarrow \qquad {}^{b}P = \begin{pmatrix} X_b \\ Y_b \end{pmatrix} = \begin{pmatrix} 1.0146 \\ -0.2966 \end{pmatrix} \text{ [m]}. \tag{8}$$

The last step requires solving the inverse kinematics of the PPR planar robot for a desired $\boldsymbol{r}_d = (p_{xd}, p_{yd}, \alpha_d)$. From the direct kinematics, one easily finds the unique solution:

$$\begin{aligned} p_x &= q_1 + \ell\cos q_3 \\ p_y &= q_2 + \ell\sin q_3 \\ \alpha &= q_3 \end{aligned} \qquad \Rightarrow \qquad \begin{aligned} q_1 &= p_{xd} - \ell\cos\alpha_d \\ q_2 &= p_{yd} - \ell\sin\alpha_d \\ q_3 &= \alpha_d. \end{aligned} \quad .$$

Setting $(p_{xd}, p_{yd}) = (X_b, Y_b)$ from (8), the desired orientation for pointing toward the origin of the camera frame 2 is computed as

$$\alpha_d = (\alpha_2 - \frac{\pi}{2}) + \text{ATAN2}\{X_2, Z_2\} - \pi = -2.4553 \text{ [rad]} = -140.68^\circ,$$

and thus $\boldsymbol{q} = (q_1, q_2, q_3) = (1.4014, 0.0902, -2.4553)$ [m, m, rad]. The solution is illustrated in Fig. 3.

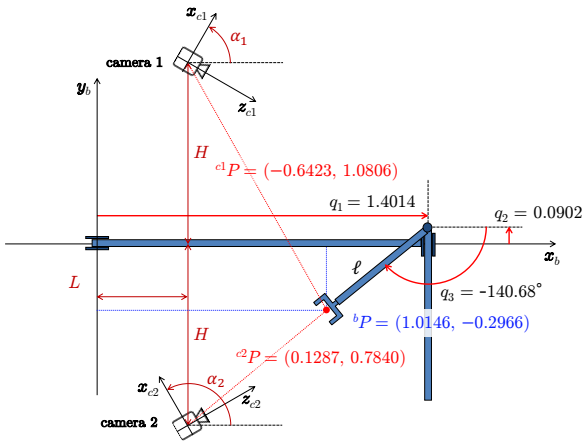

Figure 3: A graphical illustration of the solution to the visual localization and pick-up problem.

[2]The long format of MATLAB has been used to display 15 digits after the decimal point for $\boldsymbol{A}$ and $\boldsymbol{b}$. Only the first 6 are shown here.

Exercise 2

Figure 4 shows an assignment of D-H frames for the cylindrical robot that satisfies all requirements. The corresponding D-H parameters are reported in Tab. 2.

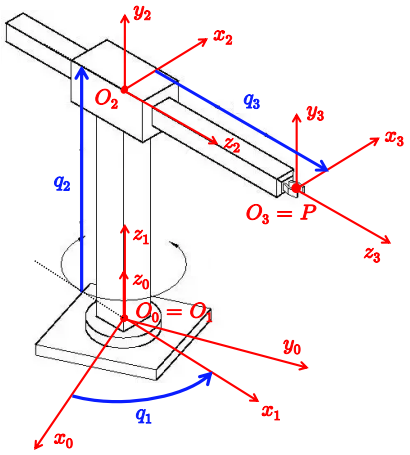

Figure 4: D-H frame assignment for the 3-dof cylindrical robot.

i	α_i	a_i	d_i	θ_i
1	0	0	0	q_1
2	$\pi/2$	0	q_2	$\pi/2$
3	0	0	q_3	0

Table 2: D-H parameters associated to the frames in Fig. 4.

The direct kinematics is computed using the elements of the D-H table as

$$ {}^0\boldsymbol{T}_3(\boldsymbol{q}) = {}^0\boldsymbol{A}_1(q_1)\,{}^1\boldsymbol{A}_2(q_2)\,{}^2\boldsymbol{A}_3(q_3) = \begin{pmatrix} -s_1 & 0 & c_1 & q_3\,c_1 \\ c_1 & 0 & s_1 & q_3\,s_1 \\ 0 & 1 & 0 & q_2 \\ 0 & 0 & 0 & 1 \end{pmatrix} = \begin{pmatrix} {}^0\boldsymbol{R}_3(q_1) & {}^0\boldsymbol{p}_3(\boldsymbol{q}) \\ \boldsymbol{0}^T & 1 \end{pmatrix}. $$

The inverse kinematics for ${}^0\boldsymbol{p}_3(\boldsymbol{q}) = \boldsymbol{p}_d = (p_{xd}, p_{yd}, p_{zd})$ is easily solved. From the third equation, one has directly

$$ q_2 = p_{zd}. $$

Squaring and summing the first two components yields the two opposite values

$$ q_3 = \pm\sqrt{p_{xd}^2 + p_{yd}^2}. $$

For each of this, provided that $q_3 \neq 0$, we obtain the other joint variable as

$$ q_1 = \mathrm{ATAN2}\left\{\frac{p_{yd}}{q_3}, \frac{p_{xd}}{q_3}\right\}, $$

with two results that differ by π. Instead, when $q_3 = 0$ one has a singular situation with q_1 remaining undefined (infinite solutions).

In the presence of the given joint limits, Fig. 5 shows the primary workspace WS_1 of the cylindrical robot. Indeed, since the third joint q_3 can never take negative values, for each $\boldsymbol{p} \in WS_1$ there is always one and only one inverse solution (no singular configurations in WS_1).

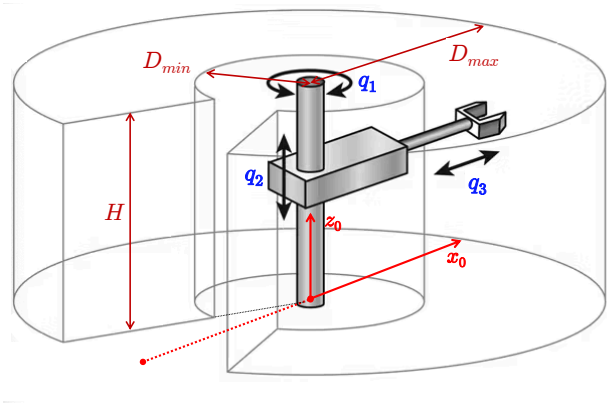

Figure 5: The primary workspace of the 3-dof cylindrical robot under the given joint limits.

The requested Jacobian is obtained by analytical differentiation of $\boldsymbol{p} = {}^0\boldsymbol{p}_3(\boldsymbol{q})$:

$$\boldsymbol{J}(\boldsymbol{q}) = \frac{\partial \boldsymbol{p}}{\partial \boldsymbol{q}} = \begin{pmatrix} -q_3\, s_1 & 0 & c_1 \\ q_3\, c_1 & 0 & s_1 \\ 0 & 1 & 0 \end{pmatrix}. \tag{9}$$

As expected, being $\det \boldsymbol{J}(\boldsymbol{q}) = q_3$, the Jacobian is singular if and only if $q_3 = 0$. In a generic singular configuration $\boldsymbol{q}_s = (q_1, q_2, 0)$, the Jacobian in (9) becomes

$$\boldsymbol{J}_s = \boldsymbol{J}(\boldsymbol{q}_s) = \begin{pmatrix} 0 & 0 & c_1 \\ 0 & 0 & s_1 \\ 0 & 1 & 0 \end{pmatrix}$$

and suitable bases for the two relevant subspaces are given by

$$\mathcal{N}(\boldsymbol{J}_s) = \text{span}\left\{ \begin{pmatrix} 1 \\ 0 \\ 0 \end{pmatrix} \right\}, \qquad \mathcal{N}(\boldsymbol{J}_s^T) = \text{span}\left\{ \begin{pmatrix} -s_1 \\ c_1 \\ 0 \end{pmatrix} \right\}. \tag{10}$$

In the first case, the physical interpretation is that any velocity of the first joint will not move the end-effector. Moreover, this property holds not only instantaneously but also over time, since a $\dot{\boldsymbol{q}}$ having only $\dot{q}_1 \neq 0$ will not let the robot escape from the singularity $q_3 = 0$. As for the null space of the Jacobian transpose in (10), when applying in the given direction a Cartesian force to the end-effector, no robot motion will result and this does not need any active counteracting joint torque by the motors; such a Cartesian force is statically balanced by the internal reaction forces of the rigid structure.

Exercise 3

Figure 6 shows the setup of the considered trajectory planning problem. The Cartesian points A and B are on the boundary (respectively, the inner and the outer) of the robot workspace. Thus, the corresponding initial and final robot configurations are singular and unique:[3] $\boldsymbol{q}_A = (\pi/2, \pi)$ and $\boldsymbol{q}_B = (0, 0)$. Nonetheless, the initial departure direction from A and the final approaching direction to B are feasible — these

[3] Joint angles are conventionally defined in the interval $(-\pi, \pi]$, open on the left and closed on the right. Therefore, we discarded the otherwise equivalent configuration $\boldsymbol{q}_A$ having $q_{A,2} = -\pi$.

directions belong to the range space of the robot Jacobian, respectively in $\boldsymbol{q}_A$ and $\boldsymbol{q}_B$. Because of these singularities, it is convenient to plan the trajectory in the joint space.

In addition, the problem requires a specific tangent direction to the joint motion in A and B, but also zero velocity at start and end (a rest-to-rest motion). Therefore, it is convenient (here, even necessary!) to split the trajectory planning problem in space (a joint-level path $\boldsymbol{q}(s)$, satisfying geometric boundary conditions) and time (a suitable rest-to-rest timing law $s(t)$).

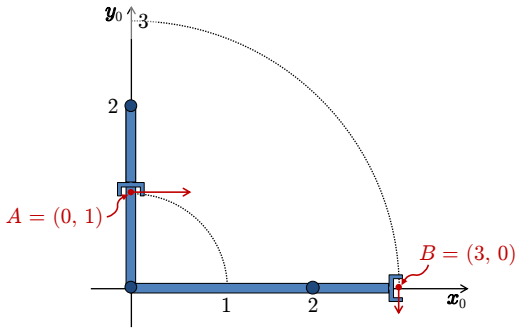

Figure 6: The considered trajectory planning problem for a 2R planar robot.

In fact, when attempting a direct solution in the time domain, we would simply use a rest-to-rest cubic trajectory for both joints, which is defined for $t \in [0, T]$ (with $T = 2$ s) in the doubly normalized form

$$\boldsymbol{q}(\tau) = \boldsymbol{q}_A + (\boldsymbol{q}_B - \boldsymbol{q}_A)\left(3\tau^2 - 2\tau^3\right), \qquad \tau = \frac{t}{T} \in [0, 1]. \tag{11}$$

The resulting trajectory and velocity of the two joints are shown in Fig. 7. Joint velocities are always negative because the two links rotate clockwise. It can be seen that both joint velocities satisfy also their feasibility bounds $|\dot{q}_1(t)| \leq V_1 = 2$ and $|\dot{q}_2(t)| \leq V_2 = 3$ [rad/s].

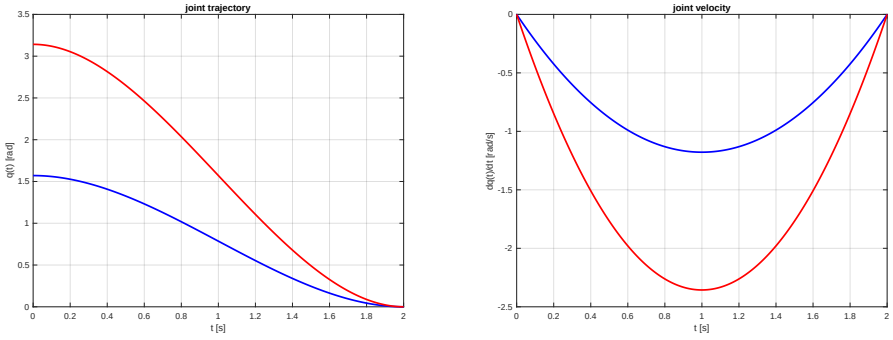

Figure 7: Rest-to-rest joint trajectory directly planned in time for $T = 2$ s, without caring about initial and final tangents to the path: joint 1 (blue), joint 2 (red).

However, when mapping the obtained joint trajectory (11) in the Cartesian space by means of the direct kinematics

$$\boldsymbol{p} = \boldsymbol{f}(\boldsymbol{q}) = \begin{pmatrix} l_1 \cos q_1 + l_2 \cos(q_1 + q_2) \\ l_1 \sin q_1 + l_2 \sin(q_1 + q_2) \end{pmatrix}, \tag{12}$$

the corresponding motion of the end-effector follows the path shown in Fig. 8. As it can be seen, the tangent to the Cartesian path at the initial point A is horizontal, but goes in the *opposite* direction[4] to the one desired, i.e., $d\boldsymbol{p}/ds|_A = (-\alpha, 0)$, for some $\alpha > 0$.

[4]When the 2R planar robot is in a singular configuration, there is only one admissible direction of instantaneous end-effector motion in the Cartesian space, characterized by a (scalable) vector in the null space of the Jacobian; nonetheless, one may exit (or enter) the singularity moving along the positive or negative direction of this vector.

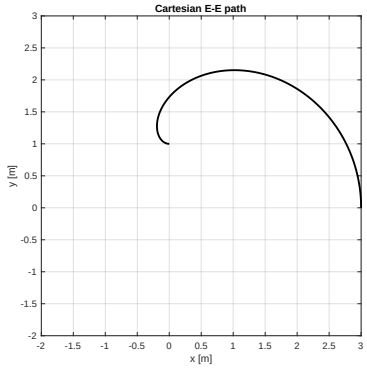

Figure 8: The Cartesian trajectory corresponding to the joint trajectory in Fig. 7.

With the above in mind, we have to the required tangent vector to the joint-space path at $\boldsymbol{q}_A$ and $\boldsymbol{q}_B$ from the given $d\boldsymbol{p}/ds|_A$ and $d\boldsymbol{p}/ds|_B$. For this, the Jacobian of the 2R planar robot

$$\boldsymbol{J}(\boldsymbol{q}) = \frac{\partial \boldsymbol{f}}{\partial \boldsymbol{q}} = \begin{pmatrix} -l_1 \sin q_1 - l_2 \sin(q_1+q_2) & -l_2 \sin(q_1+q_2) \\ l_1 \cos q_1 + l_2 \cos(q_1+q_2) & l_2 \cos(q_1+q_2) \end{pmatrix} \tag{13}$$

is evaluated at $\boldsymbol{q}_A$ and $\boldsymbol{q}_B$, yielding

$$\boldsymbol{J}(\boldsymbol{q}_A) = \begin{pmatrix} l_2 - l_1 & l_2 \\ 0 & 0 \end{pmatrix}, \qquad \boldsymbol{J}(\boldsymbol{q}_B) = \begin{pmatrix} 0 & 0 \\ l_1 + l_2 & l_2 \end{pmatrix}.$$

As anticipated, the two system of equations

$$\boldsymbol{J}(\boldsymbol{q}_A)\ \left.\frac{d\boldsymbol{q}}{ds}\right|_A = \left.\frac{d\boldsymbol{p}}{ds}\right|_A = \begin{pmatrix} 5 \\ 0 \end{pmatrix}, \qquad \boldsymbol{J}(\boldsymbol{q}_B)\ \left.\frac{d\boldsymbol{q}}{ds}\right|_B = \left.\frac{d\boldsymbol{p}}{ds}\right|_B = \begin{pmatrix} 0 \\ -1 \end{pmatrix} \tag{14}$$

are solvable, but have an infinity of possible solutions. It is convenient to choose solutions with minimum norm, because in general the larger are the initial and final values along the tangent direction to the path, the longer will be the resulting path. To obtain these minimum norm solutions, we use the pseudoinverse of the Jacobian matrices, taking into account that one has a closed-form solution for this. In fact, the following general result holds (modulo an exchange of rows):

$$\boldsymbol{J} = \begin{pmatrix} a & b \\ 0 & 0 \end{pmatrix} \qquad \Rightarrow \qquad \boldsymbol{J}^{\#} = \frac{1}{a^2+b^2} \begin{pmatrix} a & 0 \\ b & 0 \end{pmatrix}.$$

Plugging the numerical values in (14) leads to

$$\boldsymbol{q}'_A = \left.\frac{d\boldsymbol{q}}{ds}\right|_A = \boldsymbol{J}^{\#}(\boldsymbol{q}_A)\ \left.\frac{d\boldsymbol{p}}{ds}\right|_A = \begin{pmatrix} -2.5 \\ 2.5 \end{pmatrix}, \qquad \boldsymbol{q}'_A = \left.\frac{d\boldsymbol{q}}{ds}\right|_A = \boldsymbol{J}^{\#}(\boldsymbol{q}_A)\ \left.\frac{d\boldsymbol{p}}{ds}\right|_A = \begin{pmatrix} -0.3 \\ -0.1 \end{pmatrix},$$

where a prime ($'$) denotes differentiation with respect to the parameter s. Having a total of four boundary conditions for each joint, we can choose again cubic polynomials in space to solve the interpolation problem. In vector format, the joint path is defined as

$$\boldsymbol{q}(s) = \boldsymbol{a}_0 + \boldsymbol{a}_1 s + \boldsymbol{a}_2 s^2 + \boldsymbol{a}_3 s^3, \qquad s \in [0,1], \tag{15}$$

with the $\boldsymbol{a}_i \in \mathbb{R}^2$, $i = 0, \ldots, 3$, used to satisfy the boundary conditions

$$\boldsymbol{q}(0) = \boldsymbol{q}_A, \qquad \boldsymbol{q}(1) = \boldsymbol{q}_B, \qquad \boldsymbol{q}'(0) = \boldsymbol{q}'_A, \qquad \boldsymbol{q}'(1) = \boldsymbol{q}'_B. \tag{16}$$

Imposing (16), the solution is found in closed form as

$$\boldsymbol{q}(s) = \boldsymbol{q}_A + \boldsymbol{q}'_A s + \big(3(\boldsymbol{q}_B - \boldsymbol{q}_A) - (2\boldsymbol{q}'_A + \boldsymbol{q}'_B)\big)\, s^2 + \big(-2(\boldsymbol{q}_B - \boldsymbol{q}_A) + (\boldsymbol{q}'_A + \boldsymbol{q}'_B)\big)\, s^3, \tag{17}$$

with first spatial derivative

$$\boldsymbol{q}'(s) = \boldsymbol{q}'_A + \left(6(\boldsymbol{q}_B - \boldsymbol{q}_A) - 2(2\boldsymbol{q}'_A + \boldsymbol{q}'_B)\right) s + \left(-6(\boldsymbol{q}_B - \boldsymbol{q}_A) + 3(\boldsymbol{q}'_A + \boldsymbol{q}'_B)\right) s^2. \tag{18}$$

When evaluated with the given data, the general formulas (17) and (18) provide

$$\boldsymbol{q}(s) = \begin{pmatrix} 1.5708 \\ 3.1416 \end{pmatrix} + \begin{pmatrix} -2.5 \\ 2.5 \end{pmatrix} s + \begin{pmatrix} 0.5876 \\ -14.3248 \end{pmatrix} s^2 + \begin{pmatrix} 0.3416 \\ 8.6832 \end{pmatrix} s^3 \tag{19}$$

and

$$\boldsymbol{q}'(s) = \begin{pmatrix} -2.5 \\ 2.5 \end{pmatrix} + \begin{pmatrix} 1.1752 \\ -28.6496 \end{pmatrix} s + \begin{pmatrix} 1.0248 \\ 26.0496 \end{pmatrix} s^2. \tag{20}$$

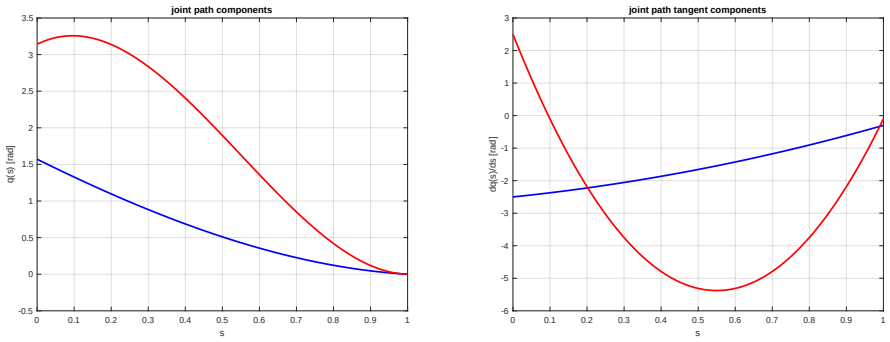

Figure 9: Components of the joint path $\boldsymbol{q}(s)$ and of its tangent vector $\boldsymbol{q}'(s)$: joint 1 (blue), joint 2 (red).

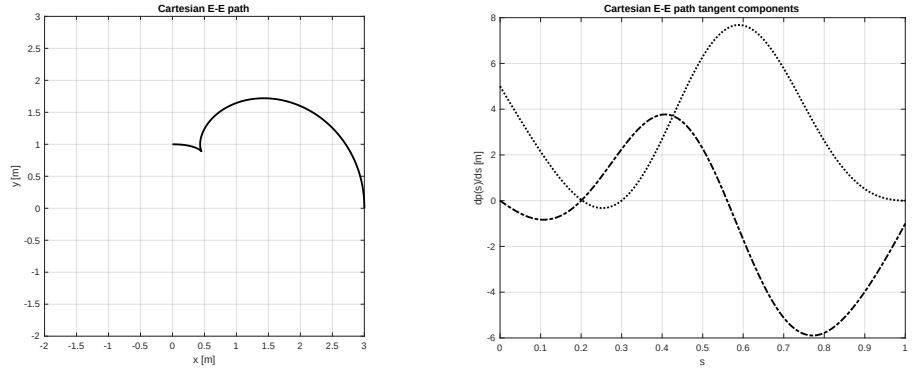

Figure 10: Path of the robot end-effector and components of its tangent vector: $p'_x(s)$ $(\cdots)$, $p'_y(s)$ $(-\cdot-\cdot)$.

Figure 9 shows the resulting path components in the joint space, as well as the components of its tangent vector. On the other hand, Fig. 10 shows the Cartesian path traced from A to B by the robot end-effector and the components of its tangent vector, as computed from the direct kinematics

$$\boldsymbol{p}(s) = \begin{pmatrix} p_x(s) \\ p_y(s) \end{pmatrix} = \begin{pmatrix} l_1 \cos q_1(s) + l_2 \cos\left(q_1(s) + q_2(s)\right) \\ l_1 \sin q_1(s) + l_2 \sin\left(q_1(s) + q_2(s)\right) \end{pmatrix} = \boldsymbol{f}(\boldsymbol{q}(s))$$

and from

$$\boldsymbol{p}'(s) = \begin{pmatrix} p'_x(s) \\ p'_y(s) \end{pmatrix} = \boldsymbol{J}(\boldsymbol{q}(s))\boldsymbol{q}'(s)$$

using the Jacobian in (13). As planned, the Cartesian path starts from A and arrives in B with the desired directions of the tangent vectors. The path has a cusp at $s = 0.2$, where $\boldsymbol{p}'(s) = \boldsymbol{0}$. Note that this occurs

even if $\boldsymbol{q}'(0.2) \neq \mathbf{0}$, because there the robot is again in a folded configuration ($q_2 = 0$ at $s = 0.2$, see Fig. 9) where the Jacobian is singular. Apparently, the vector $\boldsymbol{q}'(0.2)$ belongs to the null space of $\boldsymbol{J}(\boldsymbol{q}(0.2))$.

In order to obtain a rest-to-rest trajectory from A to B that traces the path $\boldsymbol{q}(s)$ from $s = 0$ to $s = 1$ in a given time T, we need to define a suitable timing law $s(t)$. Also in this case, the choice of a (scalar) cubic polynomial, here in doubly normalized form,

$$s(\tau) = 3\tau^2 - 2\tau^3, \qquad \tau = \frac{t}{T} \in [0, 1], \tag{21}$$

satisfies the four boundary conditions $s(0) = 0$, $s(1) = 1$, and $\dot{s}(0) = \dot{s}(1) = 0$. Figure 11 shows the profiles of the timing law $s(t)$ and of its speed $\dot{s}(t) = s'(\tau)/T = 6\tau(1-\tau)/T$ for the motion time $T = 2$ s.

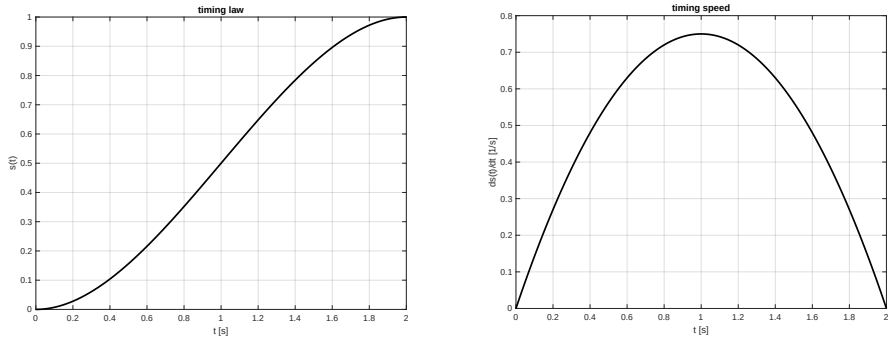

Figure 11: Rest-to-rest timing law $s(t)$ and its time derivative $\dot{s}(t)$ for a motion time $T = 2$ s.

By combining the path geometry and the timing law, we obtain the desired joint trajectory $\boldsymbol{q}_d(t) = \boldsymbol{q}(s(t))$ and its velocity $\dot{\boldsymbol{q}}_d(t) = \boldsymbol{q}'(s(t))\dot{s}(t)$, as shown in Fig. 12.

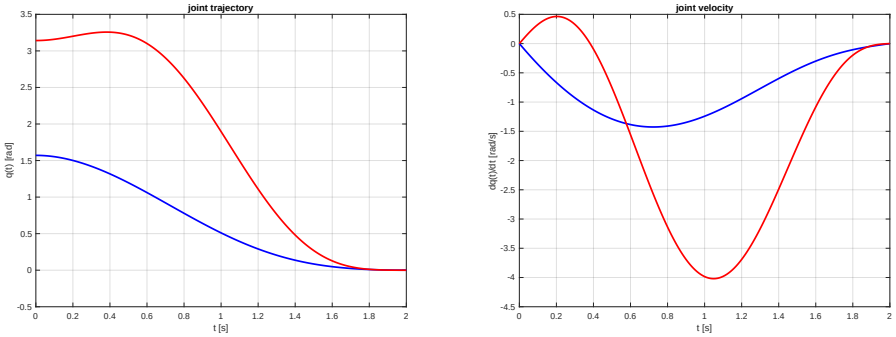

Figure 12: Joint trajectory $\boldsymbol{q}_d(t)$ and velocity $\dot{\boldsymbol{q}}_d(t)$ for motion time $T = 2$ s: joint 1 (blue), joint 2 (red).

Turning to item b), consider now the presence of the joint velocities bounds $|\dot{q}_1| \leq V_1 = 2$ and $|\dot{q}_2| \leq V_2 = 3$. From the velocity profiles in the right plots of Fig. 12, it is easy to see that both bounds are violated. However, we need an analytic verification in order to proceed (in case one has no plots).

Consider first the geometric part of the trajectory (see again Fig. 9) and compute the first and second spatial derivatives of the cubic path (15):

$$\boldsymbol{q}'(s) = \boldsymbol{a}_1 + 2\boldsymbol{a}_2 s + 3\boldsymbol{a}_3 s^2, \qquad \boldsymbol{q}''(s) = 2\boldsymbol{a}_2 + 3\boldsymbol{a}_3 s. \tag{22}$$

To find the maximum of $\boldsymbol{q}'(s)$ for each joint i, we impose

$$q_i''(s) = 0 \quad \Rightarrow \quad s_i^* = -\frac{2a_{2i}}{3a_{3i}} \quad \Rightarrow \quad q_i'(s_i^*) = a_{1i} + 2a_{2i}s_i^* + 3a_{3i}(s_i^*)^2 = a_{1i} - \frac{a_{2i}^2}{3a_{3i}},$$

or

$$q'_i(s_i^*) = q'_{Ai} - \frac{\left(3(q_{Bi} - q_{Ai}) - (2q'_{Ai} + q'_{Bi})\right)^2}{-2(q_{Bi} - q_{Ai}) + (q'_{Ai} + q'_{Bi})}.$$

Being $\boldsymbol{q}'(s)$ quadratic in s, the maximum absolute value of its components in the closed interval $[0, 1]$ is either in $s = s_i^*$, provided that $s_i^* \in [0, 1]$, or at one of the two boundaries $s = 0$ and $s = 1$. Using the numerical data, the following simple lines of MATLAB code provide the answers:

```
s_ast=-a2./(3*a3);  % here, a2 and a3 are vectors
max_dq=abs(a1-(a2.^2)./(3*a3));
for i=1,2;
  if s_ast(i) <= 0 | s_ast(i) >= 1
     max_dq(i)=max(abs(dq_A(i)), abs(dq_B(i)));
    if abs(dq_A(i)) >= abs(dq_B(i));
      s_ast(i)=0;
    else
      s_ast(i)=1;
    end
  end
end
s_ast
max_dq
```

We obtain

$$\max_{s\in[0,1]} \left|q'_1(s)\right| = |q'_1(0)| = 2.5, \qquad \max_{s\in[0,1]} \left|q'_2(s)\right| = |q'_2(0.5499)| = 5.3773,$$

in agreement with the left plots in Fig. 9.

Next, to verify the bounds on the joint velocity $\dot{\boldsymbol{q}}(t) = \boldsymbol{q}'(s(t))\dot{s}(t)$, the effect of the rest-to-rest quadratic speed $\dot{s}(t)$ of the timing law has to be included. The value $\dot{s}(0) = 0$ discards the relevance of the maximum value $q'_1(0)$ for the first joint; for this joint, one should look for the worst combination of $|q'_1(s)| \le 2.5$ in the space interval $s \in [0, 1]$ with $\dot{s}(t) \le \dot{s}_{max} = 1.5/T\,(= 0.75)$ in the time interval $t \in [0, T]$, and then compare it with the bound V_1. On the other hand, unfeasibility for the second joint can be confirmed in a more direct way. In fact, the parameter value $s_2^* = 0.5499$ at which the maximum of $|q'_2(s)|$ occurs is obtained[5] at the normalized time $\tau^* = 0.5333$ in (21), thus for $t^* = \tau^* T = 1.0666$ s; the following value violates the bound:

$$|\dot{q}_2(t^*)| = |q'_2(s_2^*)| \cdot \dot{s}(t^*) = |q'_2(0.5499)| \cdot \dot{s}(1.0666) = 5.3773 \cdot 0.7467 = 4.0150 > V_2 = 3.$$

Therefore, the motion time $T = 2$ is certainly unfeasible and the trajectory has to be slowed down.

After this (rather tedious!) verification, a convenient feasible motion time $T^* > T$ is found more directly by uniform time scaling. The only approximation introduced with respect to the minimum possible value of a feasible motion time is to attribute the maximum speed of the timing law

$$\dot{s}_{max} = \max_{t\in[0,T]} \dot{s}(t) = \dot{s}\,(T/2) = \frac{s'(0.5)}{T} = \frac{1.5}{T}$$

to the maximum absolute values of $q'_1(s)$ and $q'_2(s)$. Having already all the necessary data, we obtain

$$\begin{aligned} T^* &= 1.5 \cdot \max\left\{ \frac{\max_{s\in[0,1]} |q'_1(s)|}{V(1)}, \frac{\max_{s\in[0,1]} |q'_2(s)|}{V(2)} \right\} \\ &= 1.5 \cdot \max\left\{ \frac{|q'_1(0)|}{V_1}, \frac{|q'_2(s_2^*)|}{V(2)} \right\} = 1.5 \cdot \max\left\{ \frac{2.5}{2}, \frac{5.3773}{3} \right\} = 2.6886\,[\mathrm{s}], \end{aligned} \tag{23}$$

with $\dot{s}_{max} = 1.5/T^* = 0.5579$. The final timing law and the joint trajectory are shown respectively in Fig. 13 and Fig. 14, together with their time derivatives. While the velocity of joint 1 is well within its

[5]The cubic equation $-2\tau^3 + 3\tau^2 - 0.5499 = 0$ has just a single root $\tau^* = 0.5333$ in the interval $[0, 1]$.

bound, the maximum absolute velocity of joint 2 (which is the limiting factor) is $\dot{q}_{2,max} = 2.9903 < 3 = V_2$ — less than 1% away from the theoretical optimum. Note finally that the Cartesian path of the end-effector is still the one in Fig. 10, since time scaling does not change the geometry of the path.

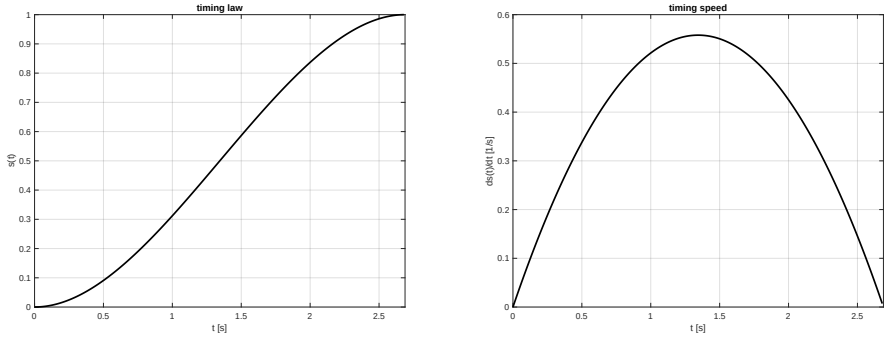

Figure 13: Rest-to-rest timing law $s(t)$ and its time derivative $\dot{s}(t)$ for a motion time $T^* = 2.6886$ s.

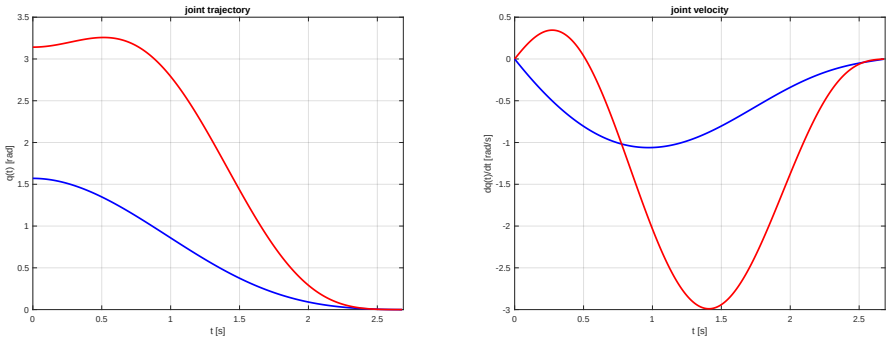

Figure 14: Joint trajectory $\boldsymbol{q}_d(t)$ and velocity $\dot{\boldsymbol{q}}_d(t)$ for motion time $T^* = 2.688$ s: joint 1 (blue), joint 2 (red).

Exercise 4

From Tab. 1, one can compute the D-H homogeneous transformation matrices of the 3R spatial robot, and from these the direct kinematics for the position of the end-effector. One has

$$\boldsymbol{p} = \begin{pmatrix} c_1(a_2c_2 + a_3c_{23}) \\ s_1(a_2c_2 + a_3c_{23}) \\ d_1 + a_2s_2 + a_3s_{23} \end{pmatrix} = \boldsymbol{f}(\boldsymbol{q}), \tag{24}$$

with the corresponding Jacobian

$$\boldsymbol{J}(\boldsymbol{q}) = \frac{\partial \boldsymbol{f}}{\partial \boldsymbol{q}} = \begin{pmatrix} -s_1(a_2c_2 + a_3c_{23}) & -c_1(a_2s_2 + a_3s_{23}) & -a_3c_1s_{23} \\ c_1(a_2c_2 + a_3c_{23}) & -s_1(a_2s_2 + a_3s_{23}) & -a_3s_1s_{23} \\ 0 & a_2c_2 + a_3c_{23} & a_3c_{23} \end{pmatrix}. \tag{25}$$

The determinant of $\boldsymbol{J}(\boldsymbol{q})$ is

$$\det \boldsymbol{J}(\boldsymbol{q}) = -a_2a_3s_3(a_2c_2 + a_3c_{23}).$$

Setting $d_1 = 0.7$ and $a_2 = a_3 = 0.5$ [m], the primary workspace of this robot is a full sphere of radius $R = a_2 + a_3 = 1$ [m], centered at $C = (0, 0, d_1) = (0, 0, 0.7)$ [m]. Singularities occur on the boundary of the sphere (where $s_3 = 0$) and along the axis of joint 1 (where $a_2c_2 + a_3c_{23} = 0$, or $p_x = p_y = 0$).

The parametric description of the desired helical path (traced for three full turns) is

$$\boldsymbol{p}_d(s) = \begin{pmatrix} r\cos 2\pi s \\ r\sin 2\pi s \\ h_0 + hs \end{pmatrix}, \qquad s \in [0,3], \tag{26}$$

with $r = 0.5$, $h_0 = 0.2$, and $h = 0.4$ [m]. The lowest point on the path is $\boldsymbol{p}_d(0) = (r, 0, h_0) = (0.5, 0, 0.2)$ [m], at a distance $\|\boldsymbol{p}_d(0) - C\| = 0.7071$ m from the sphere center C: thus, this point is inside the workspace. Similarly, the highest point $\boldsymbol{p}_d(3) = (r, 0, h_0 + 3h) = (0.5, 0, 1.4)$ is at a distance $\|\boldsymbol{p}_d(3) - C\| = 0.8602$ m from the center C of the sphere, and thus also this point belong to the reachable workspace. Moreover, being $r = 0.5 < 1 = R$, also the rest of the helical path is inside the robot workspace and no singularities are encountered.

At the initial time $t = 0$, the robot configuration and the actual end-effector position computed from (24) are, respectively,

$$\boldsymbol{q}(0) = \begin{pmatrix} 0 \\ \pi/6 \\ -\pi/2 \end{pmatrix} \text{ [rad]} \qquad \Rightarrow \qquad \boldsymbol{p}(0) = \boldsymbol{f}(\boldsymbol{q}(0)) = \begin{pmatrix} 0.6830 \\ 0 \\ 0.5170 \end{pmatrix} \text{ [m]},$$

while the desired initial position on the path (26) is

$$\boldsymbol{p}_(0) = \begin{pmatrix} 0.5 \\ 0 \\ 0.2 \end{pmatrix} \text{ [m]}.$$

We have thus an initial error

$$\boldsymbol{e}(0) = \boldsymbol{p}_d(0) - \boldsymbol{p}(0) = \begin{pmatrix} -0.1830 \\ 0 \\ -0.3170 \end{pmatrix} \text{ [m]}$$

that should be counteracted by the feedback action in the control law.

On the other hand, for a perfect tracking of the desired trajectory, the required nominal velocity command $\dot{\boldsymbol{q}}_d(t)$ (known as feedforward) is obtained by differentiating (26) with respect to the parameter s to get

$$\boldsymbol{p}'_d(s) = \begin{pmatrix} -2\pi r\sin 2\pi s \\ 2\pi r\cos 2\pi s \\ h \end{pmatrix}, \tag{27}$$

setting $s = s_d(t) = vt$, and using then $\dot{\boldsymbol{p}}_d(t) = \boldsymbol{p}'_d(s(t))\,\dot{s}(t) = \boldsymbol{p}'_d(vt)\,v$ in

$$\dot{\boldsymbol{q}}_d(t) = \boldsymbol{J}^{-1}(\boldsymbol{q}_d(t))\,\dot{\boldsymbol{p}}_d(t), \qquad \text{with } \boldsymbol{q}_d(t) = \boldsymbol{q}_d(0) + \int_0^t \dot{\boldsymbol{q}}_d(\tau)d\tau,$$

provided that the robot starts from an inverse kinematics solution $\boldsymbol{q}_d(0) = \boldsymbol{f}^{-1}(\boldsymbol{p}_d(0))$.

Since the feedback part of the control law has to react on the tracking errors expressed in the Frenet frame $(\boldsymbol{t}, \boldsymbol{n}, \boldsymbol{b})$ associated to the desired position along the path, we need to define such frame. From (27), dropping explicit dependence of terms on s, we obtain the tangent axis $\boldsymbol{t}$ of the Frenet frame as

$$\boldsymbol{t} = \frac{\boldsymbol{p}'_d}{\|\boldsymbol{p}'_d\|} = \frac{1}{\sqrt{(2\pi r)^2 + h^2}} \begin{pmatrix} -2\pi r\sin 2\pi s \\ 2\pi r\cos 2\pi s \\ h \end{pmatrix}. \tag{28}$$

Differentiating $\boldsymbol{t}$ with respect to the parameter s gives

$$\boldsymbol{t}' = \frac{\boldsymbol{p}''_d}{\|\boldsymbol{p}'_d\|} = -\frac{1}{\sqrt{(2\pi r)^2 + h^2}} \begin{pmatrix} 4\pi^2 r\cos 2\pi s \\ 4\pi^2 r\sin 2\pi s \\ 0 \end{pmatrix}, \qquad \text{with } \|\boldsymbol{t}'\| = \frac{\|\boldsymbol{p}''_d\|}{\|\boldsymbol{p}'_d\|} = \frac{4\pi^2 r}{\sqrt{(2\pi r)^2 + h^2}},$$

so that the normal axis $\boldsymbol{n}$ of the Frenet frame is

$$\boldsymbol{n} = \frac{\boldsymbol{t}'}{\|\boldsymbol{t}'\|} = \frac{\boldsymbol{p}_d''}{\|\boldsymbol{p}_d''\|} = -\begin{pmatrix} \cos 2\pi s \\ \sin 2\pi s \\ 0 \end{pmatrix}. \tag{29}$$

Finally, the third axis $\boldsymbol{b}$ of the Frenet frame is

$$\boldsymbol{b} = \boldsymbol{t} \times \boldsymbol{n} = \frac{\boldsymbol{p}_d' \times \boldsymbol{p}_d''}{\|\boldsymbol{p}_d'\| \cdot \|\boldsymbol{p}_d''\|} = \frac{1}{\sqrt{(2\pi r)^2 + h^2}} \begin{pmatrix} h \sin 2\pi s \\ -h \cos 2\pi s \\ 2\pi r \end{pmatrix}. \tag{30}$$

Note that the Jacobian matrix and all Cartesian vectors introduced so far were implicitly defined in the base frame, but without the use of a leading superscript 0. For better clarity, from now we will use where appropriate such superscripts for the reference frame of definition.

From (28)–(30), the rotation matrix that characterizes the orientation of the Frenet frame along the desired path with respect to the base frame of the robot (the 0-th frame) is

$${}^0\boldsymbol{R}_F(s) = \begin{pmatrix} \boldsymbol{t}(s) & \boldsymbol{n}(s) & \boldsymbol{b}(s) \end{pmatrix}, \qquad s \in [0, 3].$$

Let the position error with respect to the desired trajectory be expressed in the base frame and in the Frenet frame as

$${}^0\boldsymbol{e} = \begin{pmatrix} e_x \\ e_y \\ e_z \end{pmatrix} = {}^0\boldsymbol{p}_d - {}^0\boldsymbol{p} = {}^0\boldsymbol{p}_d - {}^0\boldsymbol{f}(\boldsymbol{q}), \qquad {}^F\boldsymbol{e} = \begin{pmatrix} e_t \\ e_n \\ e_b \end{pmatrix} = {}^0\boldsymbol{R}_F^T \, {}^0\boldsymbol{e}.$$

The dynamics of the position error in the Frenet frame is derived as

$$\begin{aligned} {}^F\dot{\boldsymbol{e}} &= {}^0\boldsymbol{R}_F^T \, {}^0\dot{\boldsymbol{e}} + {}^0\dot{\boldsymbol{R}}_F^T \, {}^0\boldsymbol{e} = {}^0\boldsymbol{R}_F^T \, {}^0\dot{\boldsymbol{e}} + \left(\boldsymbol{S}({}^0\boldsymbol{\omega}) \, {}^0\boldsymbol{R}_F\right)^T {}^0\boldsymbol{e} = {}^0\boldsymbol{R}_F^T \left({}^0\dot{\boldsymbol{e}} + \boldsymbol{S}^T({}^0\boldsymbol{\omega}) \, {}^0\boldsymbol{e}\right) \\ &= {}^0\boldsymbol{R}_F^T \left({}^0\dot{\boldsymbol{p}}_d - {}^0\dot{\boldsymbol{p}} - \boldsymbol{S}({}^0\boldsymbol{\omega}) \, {}^0\boldsymbol{e}\right) = {}^0\boldsymbol{R}_F^T \left({}^0\dot{\boldsymbol{p}}_d - {}^0\boldsymbol{J}(\boldsymbol{q})\dot{\boldsymbol{q}} - \boldsymbol{S}({}^0\boldsymbol{\omega}) \, {}^0\boldsymbol{R}_F^T \, {}^F\boldsymbol{e}\right), \end{aligned} \tag{31}$$

where $\boldsymbol{S}(\cdot)$ is the usual skew-symmetric matrix built with the components of its argument vector and ${}^0\boldsymbol{\omega}$ is the angular velocity of the Frenet frame moving along the path, which is extracted from

$$\boldsymbol{S}({}^0\boldsymbol{\omega}) = {}^0\dot{\boldsymbol{R}}_F \, {}^0\boldsymbol{R}_F = \begin{pmatrix} 0 & -2\pi\, v & 0 \\ 2\pi\, v & 0 & 0 \\ 0 & 0 & 0 \end{pmatrix} \qquad \Rightarrow \qquad {}^0\boldsymbol{\omega} = \begin{pmatrix} 0 \\ 0 \\ 2\pi\, v \end{pmatrix}.$$

Observing eq. (31) suggests the design of the following kinematic control law

$$\dot{\boldsymbol{q}} = {}^0\boldsymbol{J}^{-1}(\boldsymbol{q}) \left({}^0\dot{\boldsymbol{p}}_d + \boldsymbol{S}({}^0\boldsymbol{\omega}) \, {}^0\boldsymbol{e} - {}^0\boldsymbol{R}_F \boldsymbol{K}_F \, {}^F\boldsymbol{e} \right) = {}^0\boldsymbol{J}^{-1}(\boldsymbol{q}) \left(\cdots - {}^0\boldsymbol{R}_F \boldsymbol{K}_F \, {}^0\boldsymbol{R}_F^T \, {}^0\boldsymbol{e} \right), \tag{32}$$

with a suitable diagonal matrix $\boldsymbol{K}_F > 0$. The law (32) cancels all nonlinearities and couplings in the dynamics of the scalar components e_t, e_n and e_b of the error vector ${}^F\boldsymbol{e}$ in the Frenet frame, yielding

$${}^F\dot{\boldsymbol{e}} = -\boldsymbol{K}_F \, {}^F\boldsymbol{e}, \qquad \text{with } \boldsymbol{K}_F = \text{diag}\,\{2, 5, 5\} > 0,$$

so that we obtain as requested the decoupled dynamics

$$\dot{e}_t = -2e_t, \qquad \dot{e}_n = -5e_n, \qquad \dot{e}_b = -5e_b,$$

namely with exponentially converging transients.[6]

[6] The differential equation $\dot{e} = -ke$ with $k > 0$ has the solution $e(t) = e(0)\exp(-kt)$ converging to zero.

Finally, we evaluate numerically the control law (32) at $t = 0$ with the data of the problem and starting from $\boldsymbol{q}(0) = (0, \pi/6, -\pi/2)$ [rad]. The individual terms (all expressed implicitly in the base frame) are:

$$\boldsymbol{J}(\boldsymbol{q}(0)) = \begin{pmatrix} 0 & 0.1830 & 0.4330 \\ 0.6830 & 0 & 0 \\ 0 & 0.6830 & 0.2500 \end{pmatrix} = \boldsymbol{J}_0 \qquad \Rightarrow \qquad \boldsymbol{J}_0^{-1} = \begin{pmatrix} 0 & 1.4641 & 0 \\ -1.0000 & 0 & 1.7321 \\ 2.7321 & 0 & -0.7321 \end{pmatrix},$$

$$\dot{\boldsymbol{p}}_d(0) = \boldsymbol{p}_d'(0)\,\dot{s}(0) = \begin{pmatrix} 0 \\ 2\pi r \\ h \end{pmatrix} v = \begin{pmatrix} 0 \\ 3.1416 \\ 0.4 \end{pmatrix}, \qquad \boldsymbol{e}(0) = \begin{pmatrix} -0.1830 \\ 0 \\ -0.3170 \end{pmatrix}, \qquad \boldsymbol{\omega}(0) = \begin{pmatrix} 0 \\ 0 \\ 6.2832 \end{pmatrix},$$

$$\boldsymbol{S}({}^0\boldsymbol{\omega}(0))\,{}^0\boldsymbol{e}(0) = \begin{pmatrix} 0 \\ -1.1499 \\ 0 \end{pmatrix}, \qquad {}^0\boldsymbol{R}_F(0) = \begin{pmatrix} 0 & -1 & 0 \\ 0.9920 & 0 & -0.1263 \\ 0.1263 & 0 & 0.99200 \end{pmatrix},$$

and the control gain matrix

$${}^0\boldsymbol{R}_F \boldsymbol{K}_F\, {}^0\boldsymbol{R}_F^T = \begin{pmatrix} 5 & 0 & 0 \\ 0 & 2.0479 & -0.3759 \\ 0 & -0.3759 & 4.9521 \end{pmatrix}.$$

Thus, the initial value of the control command (32) is

$$\dot{\boldsymbol{q}}(0) = \begin{pmatrix} 2.7416 \\ 2.4967 \\ 1.0580 \end{pmatrix} \text{ [rad/s]}.$$

* * * * *